

Preparation, thermal insulation and flame retardance of cellulose nanocrystal aerogel modified by TiO₂

Jing Luo^{1,2}, Hua Wang^{1*}

¹ Metallurgical and Energy Engineering College, Kunming University of Science and Technology, Kunming 650093, China

² Fire Protection Institute, Southwest Forestry University, Kunming 650024, China

Corresponding Author Email: lincoln558@163.com

<https://doi.org/10.18280/ijht.360226>

ABSTRACT

Received: 10 September 2017

Accepted: 25 February 2018

Keywords:

cellulose nanocrystal (CNC), TiO₂, aerogel, flame retardance

This paper successfully prepares TiO₂-modified cellulose nanocrystal (CNC) composite aerogel through in-situ synthesis of TiO₂ in CNC solution and supercritical CO₂ drying. Then, the structure, morphology, thermal insulation and flame retardance of TiO₂/CNC composite were investigated through X-ray diffraction (XRD), scanning electron microscopy (SEM), thermogravimetry and differential thermal analysis (TG-DTA), and cone calorimeter measurement. The XRD and SEM spectra show that the TiO₂-modified CNC aerogels exhibited a 3D network structure and underwent a decline in crystallinity through TiO₂ doping and modification. The TG-DTG curves reveal that TiO₂/CNC aerogels surpassed the CNC aerogel in thermal decomposition temperature. The cone calorimeter measurement indicates that TiO₂/CNC aerogels lagged far behind the CNC aerogel in the PHRR. To sum up, the test results demonstrate that TiO₂ doping and modification is an effective way to enhance the flame retardant and thermal insulation properties of cellulose aerogel. The research findings shed new light on the development of thermal insulation and fire-retardant clothing materials.

1. INTRODUCTION

Aerogel is a synthetic porous ultralight material derived from a gel, in which the liquid component for the gel has been replaced with a gas. With excellent thermal insulation and adsorption properties, this material enjoys broad application prospects in the fields of aerospace engineering, national defence, military industry, green building and environmental governance [1]. Aerogels mainly fall into four categories, namely, inorganic aerogel, organic aerogel, carbon aerogel and composite aerogel [2]. Among them, organic aerogel has attracted more and more attention thanks to its low dielectric constant, good mechanical properties, low thermal conductivity and flexible molecular designability [3].

One of the most popular organic aerogel is cellulose aerogel, which is highly biodegradable and biocompatible. Thus, cellulose aerogel has been widely used for environmental protection. Nevertheless, cellulose aerogel is a fire hazard, i.e. it is easy to combust and release lots of toxic fumes. To avoid the hazard, many scholars have tried to improve the thermal stability and flame retardance of cellulose aerogel [4]. For instance, Wu et al. [5] prepared APP-SiO₂ aerogel/poplar fire-retardant composite by sol-gel method, and thus enhanced the thermal stability of the source material, as evidenced by the 28.1% reduction of weight loss rate at 700°C and the 5.4%~31.9% increase of the residual carbon amount. Using sol-gel method, Hribernik et al. [6] developed a layer of SiO₂ on the surface of regenerated cellulose fibres and found that the SiO₂ coating elevated the initial decomposition temperature of fibres by 20°C and pushed up the ignition and radiance temperature of the residual coke (the corresponding exothermic peak increased by 20°C~40°C).

TiO₂ is a green material with good human affinity, chemical stability, heat resistance and weather fastness [5]. The chemically-adsorbed water on the surface of TiO₂ grains can interact with the hydroxyl groups in wood cellulose, allowing the grains to deposit on wood surface or enter cell cavities and even cell walls. These grains partially block the entry of water and oxygen into wood and increase the following parameters of the wood: swelling resistance, corrosion protection, thermal stability, limiting oxygen index and burning time [6].

Using the cellulose nanocrystal (CNC) solution, this paper carries out the in-situ synthesis of TiO₂/CNC composite through the integration of aerogel preparation technique and the flame retardance principle of cellulose nanocrystal (CNC). On this basis, the TiO₂/CNC composite cellulose aerogel was prepared by supercritical CO₂ drying. Then, the author discussed the effects of TiO₂ doping and modification on the structure, morphology, thermal stability and combustion performance of cellulose aerogel, aiming to enhance the flame retardance of cellulose aerogel through TiO₂ modification. The research findings shed new light on the development of thermal insulation materials, high-temperature fire-resistant clothing materials, and high-temperature resistant equipment in China.

2. EXPERIMENT

2.1 Methodology

2.1.1 Inorganic salt induced gelation

The heavy presence of hydroxyl groups and the aggregation trend of cellulose molecules are the root causes of the conversion of cellulose solution into a gel. The gelation rate of

cellulose solution hinges on the aggregation speed of cellulose molecules. According to the principle of colloidal stability, the electrolyte has an effect on the aggregation rate of colloidal particles. If the gelation takes place in an inorganic salt solution, the charge distribution of the original sol system will be changed by the electrolyte, pushing cellulose molecules closer to form a gel. The inorganic salt can induce and promote the gelation of cellulose solution, because it disrupts the charge distribution and destroys the stability of the original sol system.

2.1.2 CNC preparation and hydrogel formation

Mix 5g poplar chips and 1.5mol/L $H_2N_2O_8S_2$ solution in a 500mL three-necked flask according to the solid-liquid ratio of 1:100 (g: mL). Stir the mixture in a water bath at 70°C for 30min. Obtain CNC through centrifuge and drying. Prepare four CNC solutions, each of which contains 10g CNC. Add TiO_2 into three of these solutions by the proportions of 1wt%, 2wt% and 3wt%, respectively. Perform ultrasonic treatment of the original CNC solution and each of the three CNC/ TiO_2 solutions in an ice bath for 15min, followed by standing for 30min. Take the suspension of each solution and add it slowly into 0.25mol/L $CaCl_2$ solution. Allow the mixed solution stand for 48h to ensure full gelation. In this way, spherical hydrogels were obtained by inorganic salt induced gelation.

2.1.3 Gel displacement

The gel displacement was conducted in multiple steps in tert-Butyl alcohol (TBA). Soak the prepared hydrogels in TBA solution (mass fraction: 25%; temperature: 40°C). Adjust the mass fraction of the TBA every 48h (50%, 75%, and 100%, respectively). Without changing the other conditions, the above procedure eventually produces spherical CNC alcogels.

2.1.4 Supercritical CO_2 drying

Supercritical CO_2 drying of the prepared CNC alcogels were performed using a supercritical fluid extractor (SFT-105, US). Heat the reactor to 40°C. Add all CNC alcogels into the reactor (atmosphere: CO_2 ; pressure: 12MPa) and dry them for 3h to obtain CNC aerogels. Denote the pure CNC aerogel, the CNC aerogel modified by 1wt% TiO_2 , the CNC aerogel modified by 2wt% TiO_2 , and the CNC aerogel modified by 3wt% TiO_2 , as S-0, S-1, S-2 and S-3, respectively.

2.2 Performance testing and characterization

Cut open the aerogel with a blade, fix it onto the sample holder with double-sided tape, and spray the sample with gold. Then, all samples were subjected to crystallinity tests using an Ultima IV X-ray diffractometer (XRD) under the following conditions: Cu-K α rays, filament current of 30mA, accelerating voltage of 40kV, scanning step length of 0.02°, scanning range of 5~40°, and scanning speed of 5°/min. The internal micro-morphology of the pure CNC aerogel and those modified with TiO_2 were observed by field emission scanning electron microscope (LEO 1530Vp, Germany).

The thermogravimetry and differential thermal analysis (TG-DTA) curve of each sample was measured by a thermogravimetric analyser (TG-209F3) in a nitrogen atmosphere at a flow rate of 30cm³/min. During the measurement, the temperature was increased from room temperature to 600°C at a heating rate of 15K/min. The thermal conductivity coefficients of all samples were determined by QTM-500 rapid thermal conductivity meter

(Xufeng, China). The cone calorimeter test was conducted on a cone calorimeter according the ISO 5660-1 standard. The sample size was 100mm×100mm×10mm, and the radiant heat flux was 30 kW/m².

3. RESULTS AND ANALYSIS

Figure 1 shows the SEM spectra of all four samples. As shown in Figure 1(a), the S-0 sample had a 3D mesh structure inside and did not collapse. During the inorganic salt induced gelation, celluloses intertwined with each other via the hydrogen bonds of hydroxyl groups, forming a 3D network with cellulose as the skeleton. Meanwhile, gas-liquid interface and surface tension were eliminated by solvent displacement and supercritical CO_2 drying, which prevents the internal structure destruction of alcogels during drying and protects the microstructure of CNC aerogel [7]. As shown in Figures 1 (b-d), TiO_2 grains were distributed inside CNC aerogel, and grew denser with the increase of the doping amount, indicating the successful doping of TiO_2 in CNC aerogel. It can be noted that S-1~3 had a different 3D network structure from the S0. This agrees well with the reduced crystallinity of S-1~3 shown by the X-ray diffraction (XRD) test.

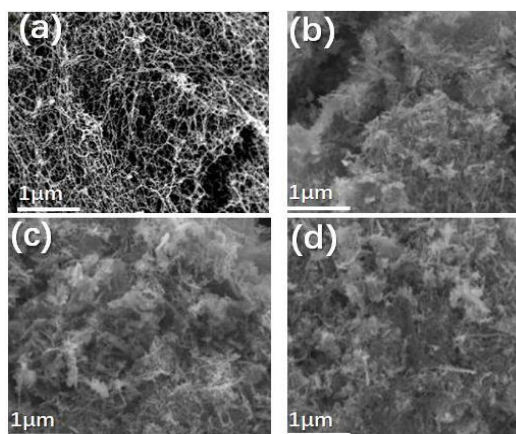


Figure 1. (a) Scanning electron microscopy (SEM) spectra of S-0 and (b-d) S1~3

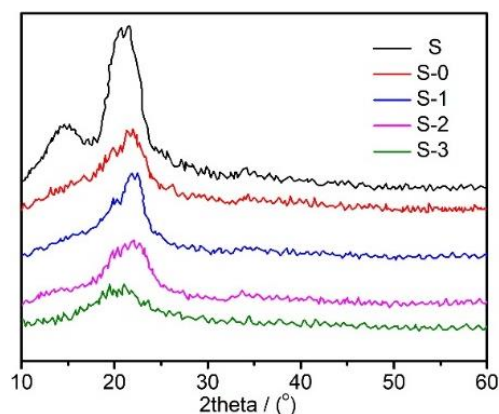


Figure 2. XRD spectra of cellulose (S) and all four samples

The XRD can characterize the crystal structure and form of CNC aerogel. The XRD spectra of cellulose (S) and all four samples (S0~4) are presented in Figure 2. It can be seen that S had two distinct diffraction peaks (15.17° and 21.22°), indicating that the crystal form of S is cellulose I crystal form.

By contrast, the diffraction peaks of S-0~4 were respectively 21.31°, 21.59°, 21.58°, and 21.02°, revealing that the cellulose loses the cellulose I crystal form after the formation of aerogel. Meanwhile, the diffraction peaks of all samples were low in intensity and relatively wide. This means the cellulose is less crystallized after aerogel formation and the crystalline area of cellulose aerogel is destroyed. The destruction can be attributed to the cellulose dissolution process in the ionic liquid during aerogel formation [8]. In addition, no TiO₂ diffraction peak was detected in the XRD test, owing to the small doping amount. Compared with the S-0, the diffraction peaks of S-1~3 were of low intensity and gradually declining with the increase of the doping amount. Thus, TiO₂/CNC aerogels are less crystallized than CNC aerogel, indicating that the crystalline area of cellulose aerogel is further destroyed after TiO₂ modification. As a result, the aerogel burns more thoroughly after pyrolysis. This can be verified by the TG test.

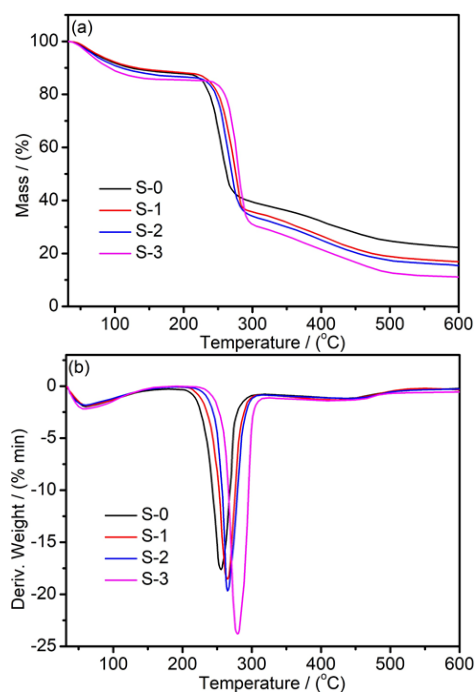


Figure 3. TG-DTG curves of all four samples

To disclose the impacts of TiO₂ doping and modification on the thermal insulation of cellulose aerogel, all four samples were subjected to the TG analysis. The resulting TG-DTG curves are recorded in Figure 3. It can be seen from Figure 3(a) that the thermal-variation of weight can be divided into three phases for all samples. In the first phase (<100°C): the mass loss of the sample is resulted from the evaporation of adsorbed moisture; in the second phase (200~350°C): the mass loss of the sample is attributable to the pyrolysis of cellulose, including the depolymerization, dehydration, and decomposition of glucose molecular chains (the end product is carbonized residue); in the third phase (>350°C): the carbonized residue was mostly oxidized and decomposed into low molecular weight gas products, and the remaining part underwent aromatic cyclization, forming the graphite structure [9,10]. Note that the second phase can be further split into two sub-phases: in 200~270°C, the alcoholic hydroxyl group was removed from the C2 position of some glucose units in the cellulose macromolecule; in 270~350°C, the alcoholic hydroxyl group was removed from the C4 position of some glucose units in the cellulose macromolecule, marking the

fracturing of glycosidic bonds. The TG curves show that the thermal decomposition temperatures of S-0, S-1, S-2, and S-3 were 213°C, 216°C, 223°C, and 239°C, respectively. Thus, TiO₂ modification can increase the thermal decomposition temperature of cellulose, promote carbon formation in the matrix and enhance the thermal stability of the composite [11].

As shown in Figure 3(b), there was a peak in each DTG curve in 200~350°C. The peak stands for the maximum weight loss rate, which corresponds to the maximum thermal decomposition rate (MTDR) temperature [12]. The MTDR temperatures of S-0, S-1, S-2 and S-3 were 255°C, 264°C, 265°C and 280°C, respectively. It can be seen that TiO₂/CNC aerogels surpassed the CNC aerogel in the MTDR temperature. Meanwhile, the MTDR of cellulose aerogel increased with the doping amount of TiO₂, revealing that the TiO₂ doping and modification can effectively elevate the MTDR temperature and enhance the thermal insulation of cellulose aerogel.

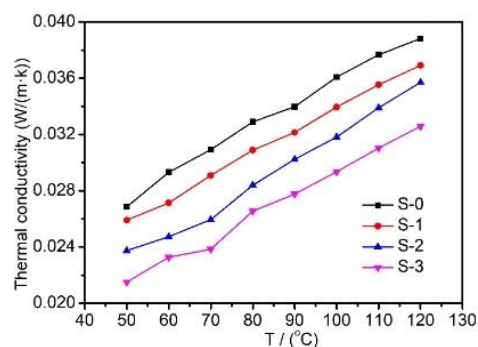


Figure 4. Thermal conductivity coefficient curves of all four samples

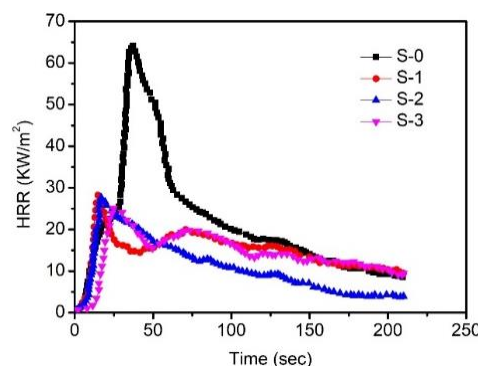


Figure 5. Heat release rate (HRR) curves of all four samples

The thermal conductivity coefficients of all samples were examined to reveal the impacts of TiO₂ doping and modification on the flame retardancy of cellulose aerogel. The resulting thermal conductivity coefficient curves are displayed in Figure 4. According to national standards, the thermal conductivity of insulation materials should be fewer than 0.174 W/(m·k) [13]. Figure 4 shows that the thermal conductivity coefficients of all four samples fell in the range of 0.002~0.004 W/(m·k). Thus, all the samples satisfy the requirements of standard insulation materials. Furthermore, S-1, S-2 and S-3 had a lower thermal conductivity than S-0, and the thermal conductivity of cellulose aerogel gradually decreased with the increase of TiO₂ doping amount. These indicate that TiO₂ doping and modification can reduce the thermal conductivity and enhance thermal insulation of cellulose aerogel. The total thermal conductivity of a material consists of solid-phase heat conduction, vapor-phase heat

conduction and radiant heat conduction. Specifically, radiant heat conduction transfers heat across separated places. The radiant thermal conductivity is negatively correlated with thermal insulation property [14]. Solid-phase heat conduction is an inherent property of all materials that changes with material density [15]. With a porous structure, TiO₂/CNC aerogels have a low density. Thus, there are many channels for heat transfer in the skeleton of the samples. Hence, the thermal conductivity of TiO₂/CNC aerogels is mainly affected by the thermal conductivity of the solid phase [16].

The HRRs of all samples were measured by the cone calorimeter to further disclose the effects of TiO₂ doping and modification on the flame retardancy of cellulose aerogel. The time-varying HRR curves of all samples are shown in Figure 5. The peak HRR (PHRR) is the key indicator of material flammability. In general, the lower the PHRR of a material, the better its flame retardance [17-21]. Figure 5 shows that the HRRs of S-0, S-1, S-2 and S-3 were 64 KW/m², 28 KW/m², 27 KW/m² and 25 KW/m², respectively. The PHRRs of S-1, S-2 and S-3 were respectively 56.25%, 57.81%, and 60.93% lower than that of S-0. The test results demonstrate that TiO₂ doping and modification can effectively reduce the HRR and enhance the flame retardance of cellulose aerogel.

4. CONCLUSIONS

This paper successfully prepares TiO₂-modified CNC composite aerogel through in-situ synthesis of TiO₂ in CNC solution and supercritical CO₂ drying, and carries out various tests on the pure CNC aerogel and CNC aerogel modified by different amounts of TiO₂. The test results show that the TiO₂-modified CNC aerogels exhibited a 3D network structure and underwent a decline in crystallinity through TiO₂ doping and modification. The TiO₂/CNC aerogels surpassed the CNC aerogel in both thermal decomposition temperature (216°C, 223°C and 239°C vs. 213°C) and MTDR (264°C, 265°C and 280°C vs. 255°C). The thermal conductivity of all cellulose aerogels meets the requirements of the national standards for thermal insulation materials. Specifically, TiO₂/CNC aerogels had a lower thermal conductivity than the CNC aerogel, and the thermal conductivity of cellulose aerogel gradually decreased with the increase of TiO₂ doping amount. Moreover, TiO₂/CNC aerogels lagged behind the CNC aerogel in the PHRR. To sum up, the test results demonstrate that TiO₂ doping and modification is an effective way to enhance the flame retardant and thermal insulation properties of cellulose aerogel. The research findings shed new light on the development of thermal insulation and fire-retardant clothing materials.

ACKNOWLEDGMENT

This work was supported financially by the Yunnan Science and Technology Plan Surface Project of China (No. 2015FB151).

REFERENCES

[1] Yuan B, Zhang J, Yu J, Song R, Mi QY, He JS, Zhang J. (2016). Transparent and flame retardant cellulose/aluminum hydroxide nanocomposite aerogels.

Science China Chemistry 59(10): 1-7. <https://doi.org/10.1007/s11426-016-0188-0>

[2] Kaya M. (2017). Super absorbent, light, and highly flame retardant cellulose-based aerogel cross linked with citric acid. *Journal of Applied Polymer Science* 134(38): 45315. <https://doi.org/10.1002/app.45315>

[3] Fan B, Chen S, Yao Q, Sun Q, Jin C. (2017). Fabrication of cellulose nanofiber/AlOOH aerogel for flame retardant and thermal insulation. *Materials* 10(3): 311. <https://doi.org/10.3390/ma10030311>

[4] Shang K, Liao W, Wang YZ. (2017). Thermally stable and flame-retardant polyvinyl alcohol/montmorillonite aerogel via, a facile heat treatment. *Chinese Chemical Letters* 29(3): 433-436. <https://doi.org/10.1016/j.ccllet.2017.08.017>

[5] Wu YQ, Tian CH, Qing Y, Yao CH, Li XG, Yang SL. (2014). Preparation and properties of APP-SiO₂ aerogel/poplar wood composite with excellent flame retardant. *Journal of Functional Materials* 45(14): 14113-14117.

[6] Hribernik S, Smole MS, Kleinschek KS. (2007). Flame retardant activity of SiO₂ -coated regenerated cellulose fibres. *Polymer Degradation & Stability* 92(11): 1957-1965.

[7] Ravi M, Samuelson L, Smith K, Westmoreland P, Parmar V, Yan F, Kumar J, Watterson A. (2008). Nanocomposites of TiO₂ and Siloxane Copolymers as Environmentally Safe Flame-Retardant Materials. *Journal of Macromolecular Science: Part A - Chemistry* 45(11): 942-946. <https://doi.org/10.1080/10601320802380208>

[8] Moafi HF, Shojaie AF, Zanjanchi MA. (2011). Flame-retardancy and photocatalytic properties of cellulosic fabric coated by nano-sized titanium dioxide. *Journal of Thermal Analysis & Calorimetry* 104(2): 717-724. <https://doi.org/10.1007/s10973-010-1133-x>

[9] Xue CH, Zhang L, Wei P, Jia ST. (2016). Fabrication of super hydrophobic cotton textiles with flame retardancy. *Cellulose* 23(2): 1471-1480. <https://doi.org/10.1007/s10570-016-0885-2>

[10] Li J, Zheng H, Sun Q, Han S, Fan B, Yao Q, Yan C, Jin C. (2015). Fabrication of super hydrophobic bamboo timber based on an anatase TiO₂ film for acid rain protection and flame retardancy. *Rsc Advances* 5(76): 62265-62272. <https://doi.org/10.1039/C5RA09643J>

[11] Vasiljević J, Tomšič B, Jerman I, Orel B, Jakša G, Simončič B. (2014). Novel multifunctional water- and oil-repellent, antibacterial, and flame-retardant cellulose fibres created by the sol-gel process. *Cellulose* 21(4): 2611-2623. <https://doi.org/10.1007/s10570-014-0293-4>

[12] Ning Y, Deng H, Ping YU. (2012). Study on nano-TiO₂ for flame-retardant finishing of cotton fabric. *Journal of Tianjin Polytechnic University*.

[13] Dogan M. (2014). Thermal stability and flame retardancy of guanidinium and imidazolium borate finished cotton fabrics. *Journal of Thermal Analysis & Calorimetry* 118(1): 93-98. <https://doi.org/10.1007/s10973-014-3950-9>

[14] Zheng Z, Liu Y, Zhang L, Wang H. (2016). Synergistic effect of expandable graphite and intumescent flame retardants on the flame retardancy and thermal stability of polypropylene. *Journal of Materials Science* 51(12): 5857-5871. <https://doi.org/10.1007/s10853-016-9887-6>

- [15] Guo L, Chen Z, Lyu S, Fu F, Wang S. (2018). Highly flexible cross-linked cellulose nanofibril sponge-like aerogels with improved mechanical property and enhanced flame retardancy. *Carbohydr Polym* 179: 333-340. <https://doi.org/10.1016/j.carbpol.2017.09.084>
- [16] Han Y, Zhang X, Wu X, Lu C. (2015). Flame Retardant, Heat Insulating Cellulose Aerogels from Waste Cotton Fabrics by in Situ Formation of Magnesium Hydroxide Nanoparticles in Cellulose Gel Nanostructures. *ACS Sustainable Chemistry & Engineering* 3(8): 1853-1859. <https://doi.org/10.1021/acssuschemeng.5b00438>
- [17] Yuan B, Zhang JM, Mi Q, Yu J, Song R, Zhang J. (2017). Transparent Cellulose-silica composite aerogels with excellent flame retardancy via in situ sol-gel process. *ACS Sustainable Chemistry & Engineering* 5(11): 11117-11123. <https://doi.org/10.1021/acssuschemeng.7b03211>
- [18] Mukherjee S, Mishra PC, Chaudhuri P, Banerjee G. (2018). Theoretical modeling and optimization of microchannel heat sink cooling with TiO₂-water and ZnO-water nanofluids. *International Journal of Heat and Technology* 36(1): 165-172. <https://doi.org/10.18280/ijht.360122>
- [19] Sun QF, Lu Y, Xia YZ, Yang DJ, Li J, Liu YX. (2012). Flame retardancy of wood treated by TiO₂/ZnO coating. *Surface Engineering* 28(8): 555-559. <https://doi.org/10.1179/1743294412Y.0000000027>
- [20] Yang YX, Zhang CY, Huang YW, Guo YS, Xu JY. (2016). The design and research of a creative automatic bouncing socket. *Mathematical Modelling of Engineering Problems* 3(2): 67-70. <https://doi.org/10.18280/mmep.030204>
- [21] He C, Huang J, Li S, Meng K, Zhang L, Chen Z, Lai Y. (2018). Mechanical Resistant and Sustainable Cellulose-based Composite Aerogels with Excellent Flame Retardant, Sound-absorption and Super-anti-wetting Ability for Advanced Engineering Materials. *ACS Sustainable Chemistry & Engineering* 6(1): 927-936. <https://doi.org/10.1021/acssuschemeng.7b03281>